Analysis of Chromate-based Primers for Protection of Aluminium Alloys on Historical Aircraft

Magali Brunet, Luc Robbiola, Chantal Brouca-Cabarrecq, Philippe Sciau

Analysis of chromate-based primers for protection of aluminium alloys on historical aircraft

Magali Brunet[a*], Luc Robbiola[b], Chantal Brouca-Cabarrecq[a], Philippe Sciau[a]

[a] *CEMES CNRS, Université de Toulouse, 29 rue Jeanne Marvig, 31055 Toulouse-France*
[b] *TRACES UT2J CNRS, Université de Toulouse, Maison de la Recherche, 31058 Toulouse-France*

Abstract:
Immediately following the use of aluminium alloys, particularly Duralumin, in the construction of aircraft, protective coatings with anti-corrosion properties were developed. Among the numerous solutions to prevent corrosion, the most widely employed materials were organic primers containing chromates. This paper reports the study of the corrosion inhibitive compounds (chromates) used by aircraft manufacturers during WWII. More specifically, we have identified the nature of the compounds and assessed their current efficiency. Our analyses on samples collected from three different wrecks- (French and German) excavated on terrestrial sites reveal that the primer contained either zinc tetroxychromate or lead chromate. Using XANES to study of the chromium oxidation states allowed to highlight the different phenomena taking place during the aging of the paint primer. We found that the reduction of Cr(VI) into Cr(III) species occurred either within the primer or at the interface of the primer with the Al alloy. This is believed to be due to alteration of the paint layer and its long exposure to natural environment. However, even after 80 years, Cr (VI) is still present in the primers of these archaeological parts. Although a little altered, the chromate compound can still provide a source of inhibitor thus maintaining the protection of the alloys.

Keywords: **Aluminium alloys, aircraft, cultural heritage, primer, chromates, XANES**

1/ Introduction

Duralumin, an alloy of aluminium with good mechanical properties (high strength and hardness), was developed by A. Wilm in 1906. The availability of this alloy gave great impetus to the general expansion of aeronautics shortly after WWI in strategic areas such as in military industry and in civil transport [1]. However, very early in the history of the alloy, the low corrosion resistance of Duralumin was a major concern and developing solutions for its protection was a priority for engineers and scientists. The corrosion inhibitive properties of chromates were well-known in the area of metal protection [2] and consequently, one of the first solutions to protect Duralumin from corrosion was the addition of chromate pigments to a paint

primer. Chromates could be associated with various cations, namely, zinc, potassium, potassium-zinc, barium, strontium, lead, etc. [3]. In parallel, different coating formulations involving chromates were also developed [4-6], such as chemical oxidation in alkaline baths (Modified Bauer and Vogel - MBV process) in the early 1920s, and soon after, chemical conversion coatings in acidic baths (also involving the use of phosphates) were reported.

Thus, the coatings present on the surface of aluminium on a historical aircraft could be very diverse and also quite complex [7]. Unfortunately, manufacturers' archives are scarce, being either lost or destroyed. It is therefore difficult to identify the nature of the anti-corrosion treatments specifically used by a nation or by an aircraft manufacturer at a particular period in history.

In the abovementioned scenario, the precise identification of the chromate-based corrosion inhibiting compound is the first step in the study of primers that have been applied on aluminium alloys in historical aircraft. This information has to be then supplemented by a detailed study of the chromium oxidation states at areas very close to the surface of the aluminium substrate so as to determine how the anti-corrosion compound changed with the passage of time. Such information could help in clarifying whether the corrosion protection provided by the chromate still remains efficient to date. This question is indeed of major importance when considering the conservation of historical aircraft, which were left for decades buried or left on the ground and so more exposed to ambient air and which might have resulted in severe degradation of the coatings to create lifting, cracks and blisters. Such degradation likely, would have affected the anti-corrosion layer too. Assessing the efficiency of the anticorrosion treatments will help in the preservation of this category of cultural heritage and in developing future restoration protocols.

Among the large corpus of WWII aircraft wrecks that we described in a previous work [8], there were only few parts that still show remains of the original paint, which make each of these painted specimen a rare testimony of this period and it is therefore important to document and preserve these samples. In this article, with the aim to extend our knowledge on the anticorrosion treatments used in the past, we collected three samples on the excavated wrecks, of which two were French aircraft (a fighter Dewoitine D.520 (1940) and a sea-plane Latécotère 298 (1940)) and the third, a German fighter aircraft, a Heinkel 111 (1937). In these samples, we have focused our investigation on the primer, *i.e.,* the first layer that is in contact with the metal and which enables the corrosion inhibitive effect. Using spectroscopic and microscopic laboratory analyses, *i.e.,* Scanning Electron Microscopy-Elemental Dispersive Spectroscopy (SEM-EDS) coupled with Raman spectroscopy, it was possible to identify the corrosion inhibitive pigment in the

primer. In addition, the oxidation state of chromium, which plays a major role in corrosion inhibition, was determined from synchrotron radiation-based techniques, *i.e.*, Micro X-Ray Fluorescence (μ-XRF) and Microscale X-ray Absorption Near Edge Structure spectroscopy (μ-XANES). The latter technique has proven to be efficient to understand chromatic alterations of yellow pigments in paintings, for example, in. Van Gogh [9] or Seurat's [10] masterpieces. In the study of anticorrosion protections of aluminium alloys, XANES has also been used to study the mechanism of action of chromate in corrosion inhibition in chemical conversion coatings (CCC) [11, 12]. In fact, hexavalent chromium Cr(VI) has a distinct pre-edge peak at 5993.5 eV linked to its tetrahedral coordination which enhances the 1s to 3d electronic transition probability. Cr(VI) can be easily distinguished from Cr(III) oxide which shows two small pre-edge peaks: a characteristic peak at 5990.5 eV and another between 5993.1 and 5994.5 eV depending on the compound [13, 14]. Another advantage of the XANES technique is that it is performed in ambient air and hence change in valence state of the active species due to high vacuum can be avoided.

In the present work, we show that depending on the manufacturer, different chromate-based pigments have been used as corrosion inhibitors on historical samples. Moreover, as it will be reported in the discussion, the characterisation of the different chemical states of chromium on each sample provides information on the alteration of the protective coatings and as to how far this protection is still effective.

2/ Materials and methods

The samples studied in this work are composed of aluminium alloys covered with a protective coating to resist corrosion (primer) on which one or more coatings of paint are present. All the samples come from wrecks excavated in the Pyrenees (South of France) and buried in a terrestrial environment. They were only brushed after excavation. The samples with residues of paint were selected after visually observing the surface of the archaeological remains. For convenience, the samples of coated aluminium alloys studied in this work are named as follows: DE520 for Dewoitine D.520, LA298 for Latécoère 298 and HE111 for Heinkel 111.

The residues of paint shown in Figure 1 are representative and characteristic of each aircraft: beige (chamois) for Dewoitine, blue for Latécoère and green for Heinkel.

Table 1 lists the elemental composition of the bulk aluminium alloy in the three samples. DE520 and the HE111 are mainly Duralumin alloys Duralumin (typically 3.5 to 5 % of Cu, 0.5 to 1% of Mg, 0.5 % of Mn and 0.5% of Si) whereas that of LA298 shows some specific differences. Although the copper and magnesium contents are close to those of Duralumin, no manganese was detected and other elements such as zinc, chromium and nickel are present in minor amounts.

<Insert Table 1 here>

Each coated sample was first observed by optical microscopy, after which, it was cut, embedded in epoxy resin and polished first on SiC papers and then on a cloth with diamond paste up to 1 µm grade to obtain a mirror-like finish. On the polished cross-sections, the coating stratigraphy could be observed by optical microscopy.

Energy Dispersive X-Ray Spectroscopy (EDS) performed on an Oxford X-Max^N 150 spectrometer, coupled to a Scanning Electron Microscope (SEM) on a FEI Helios Nanolab 600i operating at 20 kV was used to identify the elements present in the layers of paint and to determine the elemental composition of the substrate, *i.e.*, the aluminium alloy. We acquired EDS data on four 500 x 500 µm^2 areas with a minimum of 10^6 counts on each spectrum. Before each measurement, the beam intensity was optimized with respect to a pure Co standard. Quantitative analysis was performed with internal standards (pure K-line Al, Si and Fe standards) and results were normalised to 100 wt.%. Raman spectroscopy, that combines optical microscopy with spectrometry, was performed using XploRA® spectrometer from Horiba. A green laser at 532 nm was used as the excitation source. The combination of the two techniques (SEM-EDS and Raman) allowed to identify the nature of the pigments and other inorganic compounds such as fillers present in the protective coatings.

Experiments were then conducted on the same embedded samples at SOLEIL synchrotron facilities on the beamline LUCIA (Line for Ultimate Characterisation by Imaging and Absorption) using 800-8000 eV monochromatic X-ray microprobe (micron size) adapted for X-ray Absorption Spectroscopy (µ-XAS) and elemental mapping by µ-XRF. On each sample, XRF maps (each with ~ 100 µm x 50 µm area) were acquired at 6100 eV energy to locate areas containing chromium. PyMca^{TM} software was used to plot the elemental maps. Next, XANES spectra for Cr element were acquired at the points of interest (POI) that showed higher contents of Cr or across the Cr-Al interface. The acquisition was in reflection mode in the energy range from 5950 eV to 6100 eV. Energy steps were adapted to obtain well defined pre-edge peaks: 2 eV in the range 5950 eV –5986 eV (below the pre-edge peak), 0.2 eV in the range 5986 eV – 6014 eV (around the pre-edge peak), 0.5 eV in the 6014 eV – 6040 eV and 1 eV up to 6100 eV. After acquisition, the spectra were normalised using the Demeter^{TM} suite (Athena^{TM} software).

3/ Results

3.1. General observations and identification of corrosion inhibiting compounds

Initial macroscopic observation on the surface of all the samples (see Figure 1) highlights alterations in the paint layers which present cracks, blisters and delamination. Such alterations are mainly linked to their aging (> 80 years). On the outermost surface of the sample HE111, concretions are also present, due to its buried state.

Figure 2 and 3 present the images and analyses acquired by optical microscopy and SEM-EDS on the cross-sections of the three samples. For all the samples, the primer is the red layer that is in direct contact with the aluminium alloy. The SEM-EDS study showed that for the two French aircraft (DE520 and LA298), Cr element is associated with Zn and K inside the red primer layer forming the pink species in the EDS maps of the Figures 2a and b. On LA298, a thin layer of Cr only correlated to O was homogeneously distributed on the surface of the alloy over the entire sample. As for the paint layers, both DE520 and LA298 samples contain Ti-O (TiO_2) as a mineral filler. Cr was also found in the paint layer of LA298 associated with Pb and O.

<Insert Figure 2>

The sample HE111 is composed of 4 layers as seen in Figure 1.c: the red primer, a metallic grey layer (hereafter denoted as layer 1), a light green layer and a darker green layer. Two representative zones were studied: zone H1 reported in Figure 3.a, where only the red primer and the metallic grey layer (layer 1) are conserved and in Figure 3.b, the zone H2, where the primer is not clearly observed with a concretion layer replacing the primer/paint. The EDS mapping on zone H1 (see Figure 3.a), shows that the red primer contains micron-size platelets (parallel to the surface) with Si, Mg and O elements. This compound was identified as talc based on X-ray diffraction data (not reported here), a common mineral filler used by German manufacturers. Three submicronic phases were also detected containing: Cr-O-Pb (corresponding to the inhibitive pigment), Fe-O, and Zn-O elements. Between the two zones, H1 (with primer and paint) and H2 (with only the concretion layer), we performed EDS mapping, shown in Figure 3.b, to reveal the transition between the two zones. Our results revealed that the concretion layer is composed of three phases of different elemental composition including: K-Si-O, Si-O, and Fe-O or Ca-Al-O (probably from the soil). In the zone H2, Cr element was only rarely present and in very few areas underneath the concretion layer.

<Insert Figure 3>

We used Raman spectroscopy to identify chromate-containing crystals both in the primer and the paint layer. As shown in the spectra of Figure 4.a, the pigment $4ZnCrO_4.K_2O.3H_2O$ (zinc tetroxychromate) was identified in the primer present in the two French aircraft samples (DE520 and LA298): the strong peak at 872 cm^{-1} corresponds to the CrO_4 group (ν_1) stretching. Other peaks at 343m, 357w (shoulder), 372 w, 407w, 771w, 892m and 941m cm^{-1} are also typical of this compound [15]. Zinc tetroxychromate ($4ZnCrO_4 \cdot K_2O \cdot 3H_2O$) is a well-known pigment that was developed in the 19th century [16]. This compound was tested as a corrosion inhibitive pigment in the early 1940s [2] and proved to be an excellent inhibitor as well as being resistant to humidity. Hence, it has been widely used in aeronautics industry as corrosion inhibitor for aluminium alloys, particularly in France [5, 17]. The red colour of the primer was attributed to the presence of Fe_2O_3 (hematite). On the sample LA298, due to the very small thickness of the Cr-O layer, no Raman spectrum could be collected at the interface.

In the sample HE111, as shown in the Figure 4.b, the identified Cr-compound in the primer was $PbCrO_4$ (crocoite). A main peak is found around 835 cm^{-1} corresponding to the stretching (ν_1) of the CrO_4 group in lead chromates, as for instance, crocoite. The other peaks at 334, 355, 373 and 397 cm^{-1} confirm the identification of crocoite [18, 19]. Compared to zinc chromates, the CrO_4 stretching mode in crocoite is shifted to a lower wavenumber of 837 cm^{-1} due to the presence of PbO [15].

It should be pointed out here that in the LA298 paint layer, lead chromate ($PbCrO_4$) was also identified as the yellow pigment.

<Insert Figure 4>

3.2. XANES investigation on cross-sections

Figure 5 shows the XRF maps and XANES data for the DE520 sample. A tri-colour (Ti, Cr, Al) map was chosen in order to visualize the interfaces (substrate/primer/paint) and select the point of analyses. XANES was acquired on a line profile crossing the primer, from the points of interest POI 09 to POI 14 with steps of 2 µm in the Z direction. As shown in Figure 5.b, all the XANES spectra are similar with a sharp pre-edge peak at 5993 eV. The height of the normalised pre-edge peak ($H_{\mu(5993)}$) can be directly correlated to the proportion of Cr(VI) in the total chromium content which, as proposed by Zanella *et al.* [10], follows the equation: $H_{\mu(5993)} = (0.95 \pm 0.01) * x$, where x represents the fraction [Cr(VI)/Cr total]. We have plotted the reference sample with 100%

Cr(VI) corresponding to Zn yellow ($K_2O.4ZnCrO_4.3H_2O$) used by Zanella *et al.* along with our spectra. For the reference sample, the height of the normalised pre-edge peak ($H_{\mu(5993)}$) is very close to 1. For the spectra measured on DE520, the height of the pre-edge peak lies between 0.78 and 0.84 indicating the predominant presence of Cr(VI)-containing species with a small amount of Cr(III) species. The rest of the spectra (from 5594 eV to 6020 eV) is in good agreement with that observed for the reference sample with 75% Cr(VI) : 25% Cr(III) reported by the same authors [10].

<Insert Figure 5>

Similar XRF maps were acquired for the LA298 sample, (see Figure 6.a). The XANES spectra measured across the primer: from POI 10 to POI 23 (with a step of 1 µm) together with the reference Zn yellow spectrum are plotted in Figure 6.b. An additional spectrum for POI 06 showing a typical Cr(0) (chromium metal) behaviour was acquired. This clearly confirms the presence of Cr as a minor element (i.e. higher than 0.1 wt.%) in the alloy as determined from the SEM-EDS analysis (Table 1). Next, on the profile line of the primer from POI 10 to POI 23, a mixture of Cr(III) and Cr(VI) was found. Figure 7 plots the Cr(VI) intensity over the maximum intensity extracted from the reference Zn yellow spectrum ($H_{\mu(5993)}$) versus the distance (in micrometre): POI 10 corresponds to 0 µm and POI 23 to 13 µm. This shows that at the interface with the metal, the Cr(III) content is significantly greater than Cr(VI), *i.e.* Cr(VI)/ Cr total~ 0.25; the Cr(VI) content increases reaching a maximum with a ratio of 0.67 in the primer layer at the interface with the paint. A lower height of the Cr(VI) peak is observed in the paint, with a normalised intensity around 0.5, related to the change of cation in the chromate compound (zinc chromate => lead chromate) earlier identified by Raman spectroscopy.

<Insert Figure 6 and 7>

For the HE111 sample, different elements were chosen to construct tri-colour maps of the interfaces, as shown in Figures 8.a and 9.a.These include Al, Cr, and Si for the H1 zone, Si being representative of talc which is largely present in layer 1, and Al, Cr, and Ca for the H2 zone since Ca is one of the elements present in the concretion layer.

For the H1 zone where the primer is still present, as shown in Figure 8, the XANES spectra across the primer interface (from POI 09 to POI 13, step 2 µm) exhibit the same behaviour all the way from the alloy up to the concretion layer (see Figure 8.b) showing a mixture of Cr(III)

and Cr(VI) with Cr(VI) being preponderant; the height of the pre-edge peak ($H_{\mu(5993)}$) on the normalised spectrum was between 0.6 and 0.7.

<Insert Figure 8>

For the H2 zone, Figure 9.b shows the XANES spectra in the primer, from POI 01 to 05 (with steps of 3 µm). The spectra have a totally different shape to those of the H1 zone. Two pre-edge peaks at 5990.6 eV and 5993.5 eV are seen, evidencing the presence of a mixture of Cr(III) and Cr(VI), but with Cr(III) being predominant. The height of the first pre-edge peak appears to vary but this trend is not correlated to the distance of the POI from the interface primer/alloy.

<Insert Figure 9>

As compared to reported XANES spectra for Cr_2O_3 reported in the literature [9, 10, 13], the spectra acquired in this H2 zone present significant differences. The usually reported second pre-edge

peak at 5994.5 eV is not present (see insert of Figure 9.b) and the post-edge shapes do not match. On the other hand, the XANES shape is similar to that previously reported for $Cr(OH)_3$ [14, 20] indicating that the Cr(III) compound detected in the present case is not an oxide of chromium oxide but rather a hydroxide.

4/ Discussion

The analysis of the three primers applied on WWII aircraft by spectroscopic and microscopic techniques (SEM-EDS coupled with Raman) allowed to identify two corrosion inhibitive pigments, namely, zinc tetroxychromate ($K_2O.4ZnCrO_4.3H_2O$) for the two French aircraft (DE520 and LA298) and lead chromate ($PbCrO_4$) for the German aircraft (HE111). From XANES measurements across the interfaces of the investigated samples, we identified three different oxidation states of chromium, namely, Cr(0), Cr(VI) and Cr(III)).

We noted several cases where Cr(III) species was present locally. First, in the DE520 sample, a small proportion of Cr(III) with mainly Cr(VI) was found across the primer thickness (Figure 5), which we believe, is linked to the degradation of chromate within the primer, as already shown in another reported work [9]. In the LA298 sample, a similar process was observed in the paint layer. The pre-edge peak intensity of around 0.5 for Cr(VI) in the paint layer could be due to an alteration of the chromate compound.

At the primer/Al alloy interface of the LA298 sample, as evidenced in Figure 6, Cr(III) is clearly present forming a thin internal sub-layer of the primer. No signal was found in Raman spectra taken in this zone to substantiate this conclusion, but the sensitivity of the Raman signal for Cr(III) is known to be lower than for Cr(VI) [21]. It is possible that different types of Cr(III) compounds were present. From the XANES spectra (Figure 6), we infer that chromium oxide (Cr_2O_3) is not prevalent but instead, a complex form such as chromium hydroxide is more likely to be present. Considering that this Cr(III)-containing sub-layer is homogeneous on the sample and within a primer that has remained intact but mainly containing Cr(VI), several hypotheses can be made. The presence of the Cr(III)-containing sub-layer could be due either to a specific treatment applied prior the deposition of the primer such as a flash primer, or to a process similar to chromate conversion coatings (CCC). The second possibility is that the primer/paint layers were degraded due to ageing during the long period of time the wreck was on the ground and exposed to the elements. In this ageing process, the penetration of humidity could have occurred first uniformly across the paint layer and then the primer, inducing leaching of Cr(VI) oxyanions from the primer. Subsequently, the following reactions are possible, as already reported in [11, 21, 22]: migration of the chromate species (CrO_4^{2-}, $HCrO_4^-$ or $Cr_2O_7^{2-}$

depending on the pH) and its adsorption on the active corrosion sites of aluminium (pits). In contact with the $Al(OH)_x$ at the surface and through the release of H^+, the chromium species could then be reduced to the trivalent form, eventually resulting in a Cr(VI)/(Cr(III) mixed oxide at the metal surface.

For the HE111 sample, as observed by OM (Figure 3), the painting system (primer, paint) is altered, with the creation of lacunae and concretions. In the H1 zone, where the primer and one paint layer are still present, the XANES spectra (see Figure 8.b) show that chromate is still in the form of Cr(VI), with a small proportion of Cr(III and only a minor alteration in composition is seen. In the H2 zone where Ca-containing concretions covered the alloy surface, Cr element was only rarely spotted by SEM-EDS (see map of Figure 3.b) but was detected by µ-XRF, as shown in Figure 9.a. This proves that the primer was originally present and it underwent a chemical reaction. XANES spectra indicate the predominance of Cr(III). Thus, it is possible that, similar to the LA298 sample, even after the disappearance of the physical protective coating provided by the paint layer and the primer, Cr(VI) originally present in the lead chromate pigment still effectively played its role as a corrosion inhibitor. Cr(VI) locally reacted with the aluminium substrate in the presence of ambient humidity producing chromium hydroxide Cr(III) at the alloy interface. This type of reaction has been experimentally demonstrated in the case of CCC on Al 2024T3 alloy [12] and for a chromate-containing protective paint system on the Al 2024-T3 alloy [23], which are in good concordance with the result obtained on coated duralumin samples that have naturally aged from WWII times.

Conclusions

A study of the chromate compounds found in the primers applied on Al alloys present in three different WWII aircraft was done combining SEM-EDS analysis, Raman spectroscopy, µ-XRF and XANES. From the results on sample cross-sections, several conclusions can be made:

- In the two French aircraft, the Dewoitine D.520 (1940) and the sea-plane Latécoère 298 (1940), the corrosion inhibitive pigment in the primer was the well-known zinc tetroxychromate ($4ZnCrO_4 \cdot K_2O \cdot 3H_2O$), also used as a yellow pigment in contemporary paints. On the German aircraft, Heinkel 111 (1937), the pigment used for its anticorrosion properties was lead chromate ($CrPbO_4$).

- For all the three aircraft, inside the primer layer and when the primer was still covered with a paint layer, chromium was still hexavalent Cr(VI) but with a small proportion of trivalent chromium Cr(III). It is known that the slightly soluble hexavalent chromium provides a continuous timed-release of inhibitor [6]. Thus, we can deduce that after exposure to outdoor

environment or buried for 80 years, although the chromate pigment is slightly altered, the corrosion inhibition properties of the primer are most probably maintained.

- On the other hand, wherever the coating is no longer a primer/paint layer, *e.g.*, in the case of areas deficient in paint or lacunas as shown on the Heinkel aircraft, large amounts of Cr(III) species were found. This indicates that mostly all the Cr(VI) was reduced to Cr(III) species, forming a Cr(III) film (probably chromium hydroxide) which inhibited oxygen reduction (cathodic partial reaction). This Cr(III) film having a permanent corrosion inhibiting activity [22], it can be argued that passivation was ensured and the original aluminium substrate was still protected from corrosion.

However, to confirm these results, the corrosion inhibition efficiency of these old primers should be tested in laboratory experiments, *i.e.*, in controlled corrosive environments simulating atmospheric conditions.

Acknowledgments

The samples were provided by the association Aérocherche for which we extend our special thanks to Gilles Collaveri. We also acknowledge SOLEIL for providing synchrotron radiation facilities and Delphine Vantelon for assistance in using the beamline LUCIA (Proposal 20200361). We would also like to thank Jean-François Gaillard who kindly provided the reference XANES spectrum of Zinc Yellow.

References:

[1] J. Carpentier, *Cent vingt ans d'innovations en aéronautique*, Hermann ed., 733 p., France, 2011.

[2] W. W. Kittelberger, "Zinc tetroxy chromate, a rust-inhibitive primer pigment," *Industrial and engineering chemistry,* vol. 34, no. 3, pp. 363-372, 1942.

[3] H. G. Cole, "Tests on the relative efficiency of chromate pigments in anticorrosive primers," *Journal of applied chemistry,* vol. 5, pp. 197-208, 1955.

[4] C. Adams, and D. Hallam, "Finishes on aluminium - a conservation perspective," in Symposium '91: Saving the twentieth century, Ottawa, Canada, 1991, pp. 273-286.

[5] P. Rousset-Bert, "La protection des structures en métal léger dans la construction aéronautique," *Corrosion et Anticorrosion,* vol. 6, no. 9, pp. 74-89, 1958.

[6] M. W. Kendig, and R. G. Buchheit, "Corrosion Inhibition of Aluminum and Aluminum Alloys by Soluble Chromates, Chromate Coatings, and Chromate-Free Coatings," *Corrosion,* vol. 59, no. 5, pp. 379-400, 2003.

[7] K. A. Merrick, and J. Kiroff, *Luftwaffe camouflage and markings 1933-1945*: Ian Allan Publishing, 2010.

[8] T. Ouissi, G. Collaveri, P. Sciau *et al.*, "Comparison of Aluminum Alloys from Aircraft of Four Nations Involved in the WWII Conflict Using Multiscale Analyses and Archival Study," *Heritage,* vol. 2, no. 4, 2019.

[9] L. Monico, K. Janssens, M. Alfeld *et al.*, "Full spectral XANES imaging using the Maia detector array as a new tool for the study of the alteration process of chrome yellow pigments in

paintings by Vincent van Gogh," *Journal of Analytical Atomic Spectrometry,* vol. 30, no. 3, pp. 613-626, 2015.

[10] L. Zanella, F. Casadio, K. A. Gray *et al.*, "The darkening of zinc yellow: XANES speciation of chromium in artist's paints after light and chemical exposures," *Journal of Analytical Atomic Spectrometry,* vol. 26, no. 5, pp. 1090-1097, 2011.

[11] M. W. Kendig, A. J. Davenport, and H. S. Isaacs, "The mechanism of corrosion inhibition by chromate conversion coatings from X-ray absorption near edge spectroscopy (Xanes)," *Corrosion Science,* vol. 34, no. 1, pp. 41-49, 1993.

[12] N. Le Bozec, S. Joiret, D. Thierry *et al.*, "The Role of Chromate Conversion Coating in the Filiform Corrosion of Coated Aluminum Alloys," *Journal of The Electrochemical Society,* vol. 150, no. 12, pp. B561, 2003.

[13] L. Monico, K. Janssens, M. Cotte *et al.*, "Chromium speciation methods and infrared spectroscopy for studying the chemical reactivity of lead chromate-based pigments in oil medium," *Microchemical Journal,* vol. 124, pp. 272-282, 2016.

[14] L. Monico, M. Cotte, F. Vanmeert *et al.*, "Damages Induced by Synchrotron Radiation-Based X-ray Microanalysis in Chrome Yellow Paints and Related Cr-Compounds: Assessment, Quantification, and Mitigation Strategies," *Analytical Chemistry,* vol. 92, no. 20, pp. 14164-14173, 2020.

[15] I. M. Bell, R. J. H. Clark, and P. J. Gibbs, "Raman spectroscopic library of natural and synthetic pigments (pre- ≈ 1850 AD)," *Spectrochimica Acta Part A: Molecular and Biomolecular Spectroscopy,* vol. 53, no. 12, pp. 2159-2179, 1997.

[16] V. Otero, M. F. Campos, J. V. Pinto *et al.*, "Barium, zinc and strontium yellows in late 19th–early 20th century oil paintings," *Heritage Science,* vol. 5, no. 1, pp. 46, 2017.

[17] J.-J. Meynis de Paulin, "La peinture de l'aluminium - Part 2," *Revue de l'Aluminium n°138*, no. 138, pp. 325-331, Novembre 1947.

[18] R. L. Frost, "Raman microscopy of selected chromate minerals," *Journal of Raman Spectroscopy,* vol. 35, no. 2, pp. 153-158, 2004.

[19] L. Burgio, and R. J. H. Clark, "Library of FT-Raman spectra of pigments, minerals, pigment media and varnishes, and supplement to existing library of Raman spectra of pigments with visible excitation," *Spectrochimica Acta Part A: Molecular and Biomolecular Spectroscopy,* vol. 57, no. 7, pp. 1491-1521, 2001.

[20] N. Papassiopi, F. Pinakidou, M. Katsikini *et al.*, "A XAFS study of plain and composite iron(III) and chromium(III) hydroxides," *Chemosphere,* vol. 111, pp. 169-176, 2014.

[21] J. Zhao, G. Frankel, and R. L. McCreery, "Corrosion Protection of Untreated AA-2024-T3 in Chloride Solution by a Chromate Conversion Coating Monitored with Raman Spectroscopy," *Journal of The Electrochemical Society,* vol. 145, no. 7, pp. 2258-2264, 1998.

[22] G.S. Frankel, Mechanism of Al alloy corrosion and the role of chromate inhibitors, OHIO STATE UNIV COLUMBUS FONTANA CORROSION CENTER, 2001.

[23] S.A. Furman, F.H. Scholes, A.E. Hughes, D.N. Jamieson, C.M. Macrae, A.M. Glenn, "Corrosion in artificial defects. II. Chromate reactions", *Corrosion Science,* vol. 48, no. 7, pp. 1827-1847, 2006

Table 1. Elemental composition in normalised weight (wt.%) measured by SEM-EDS analysis on polished cross-sections (estimated error is 10% for minor elements).

Figure 1. Optical microscopy images of the paints on each of the samples: a) DE520, b) LA298, c) HE111.

Figure 2. Protective coating of samples a) DE520 and b) LA298 in cross-section: optical microscopy images (left column), SEM-BEI images (middle column) and SEM-EDS mapping (right column) with Cr (dark blue), Zn (red magenta), Fe (green), Al (yellow), K (orange) and Ti (light blue).

Figure 3. Protective coating of sample HE111 in cross-section observed by optical microscopy and analysed by SEM-EDS, showing a) zone H1. *Inset:* EDS maps with Cr (dark blue), Zn (red magenta), Fe (green), Al (yellow), Pb (orange), Si (light blue) and b) intermediate zone between H1 and H2 zones. *Inset:* EDS maps with additional elements K (red), Ca (turquoise).

Figure 4. Raman spectrum on a crystal in the primer layer of a) DE520 and LA298 samples and b) HE111 sample

Figure 5. DE520 cross-section sample: a) XRF (Cr, Ti, Al) map revealing the paint layer (green) and the primer (red) on the Al alloy (blue), with POI profile line (from 09 to 14) and b) the corresponding normalised XANES spectra across the Al/primer interface; *inset*: close-up view of the pre-edge peak at 5993.5 cm^{-1}. Spectrum of the reference zinc yellow pigment $K_2O*4ZnCrO_4*3H_2O$ (courtesy of J.F. Gaillard) is also shown (dashed line).

Figure 6. LA298 cross-section sample: a) XRF (Cr, Ti, Al) map with POI 06 (in the Al alloy) and POIs from 10 to 23; b) Normalised XANES spectra across the Al/primer interface:), POI 06 (Al alloy), POI 10-POI 11 (interface); POI 14 (in the middle of the layer) plotted together with that of the reference Zn yellow (dashed line); *inset:* close-up view of the pre-edge peak.

Figure 7. LA298 cross-section sample - Evolution of the Cr(VI) peak intensity at 5993.5 eV normalised to (Cr total) ($H_{\mu(5993)}$) within the primer from POI 10 (0 µm) to POI 23 (13 µm).

Figure 8. HE111-zone H1 cross section sample: a) XRF (Cr, Si, Al) map with POIs from 09 to 13; b) normalised XANES spectra across the Al/primer interface. The plot for the reference Zn yellow is shown by the dashed line; Inset: close-up view of the pre-edge peak.

Figure 9. HE111-zone H2 cross-section sample: a) XRF (Cr, Ca, Al) map with POIs from 01 to 05 and b) normalised XANES spectra across the Al/concretion interface; *Inset:* close-up view of the pre-edge peaks.

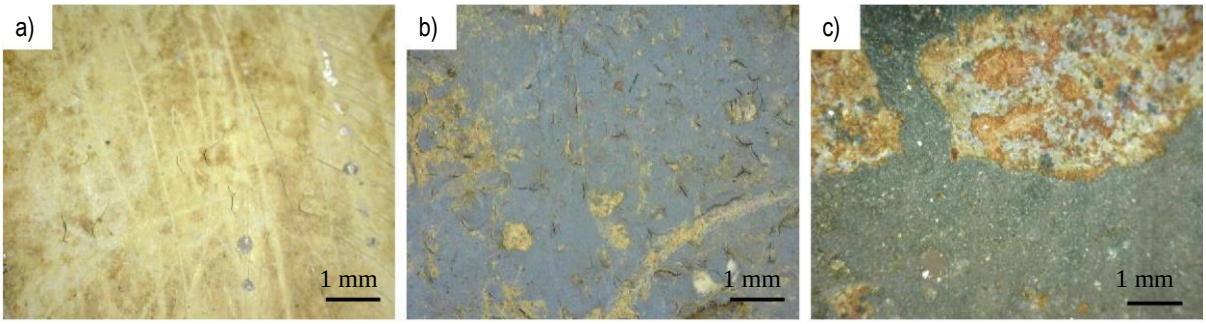

Figure 1. Optical microscopy images of the paints on each of the samples: a) DE520, b) LA298, c) HE111.

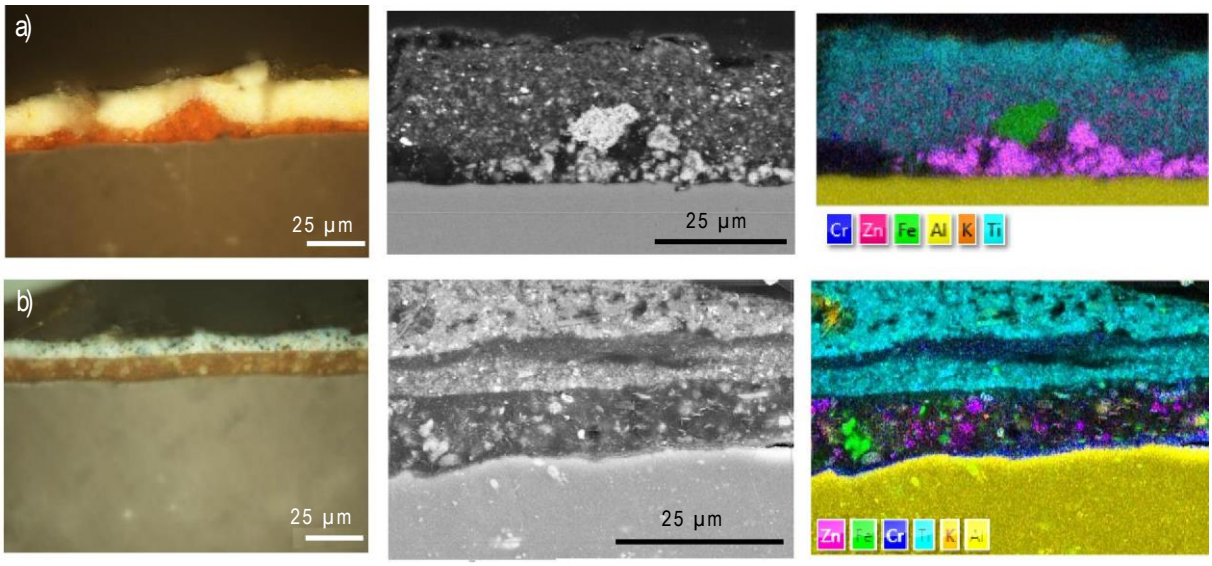

Figure 2. Protective coating of samples a) DE520 and b) LA298 in cross-section: optical microscopy images (left column), SEM-BEI images (middle column) and SEM-EDS mapping (right column) with Cr (dark blue), Zn (red magenta), Fe (green), Al (yellow), K (orange) and Ti (light blue).).

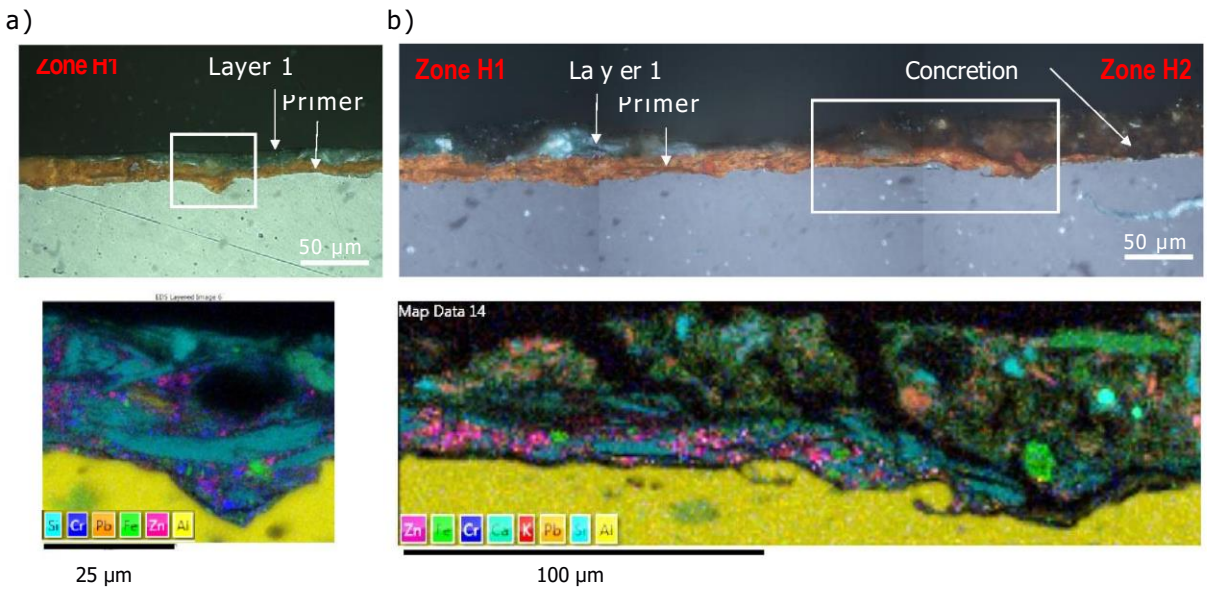

Figure 3. Protective coating of sample HE111 in cross-section observed by optical microscopy and analyzed by SEM-EDS, showing a) zone H1. Inset: EDS maps with Cr (dark blue), Zn (red magenta), Fe (green), Al (yellow), Pb (orange), Si (light blue) and b) intermediate zone between H1 and H2 zones. Inset: EDS maps with additional elements K (red), Ca (turquoise).

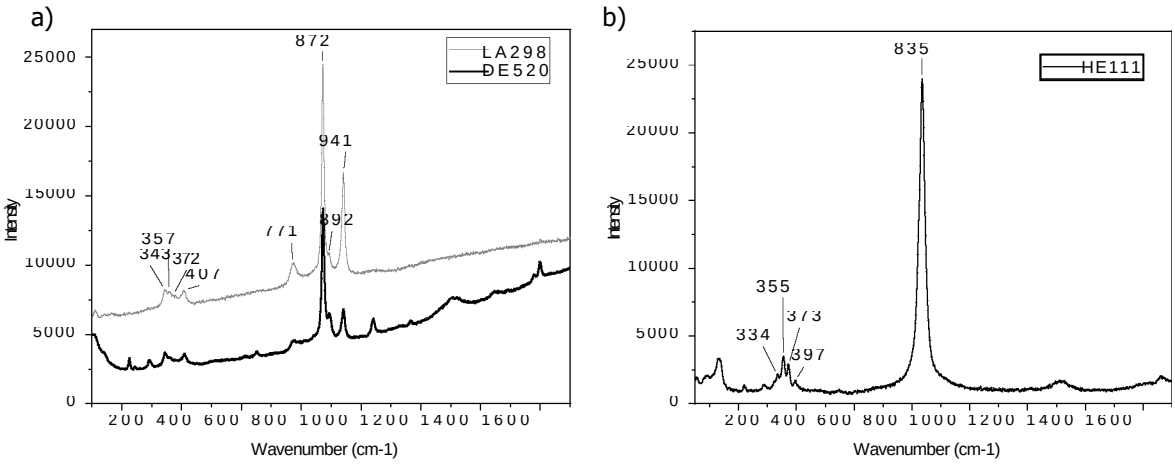

Figure 4. Raman spectrum on a crystal in the primer layer of a) DE520 and LA298 samples and b) HE111 sample

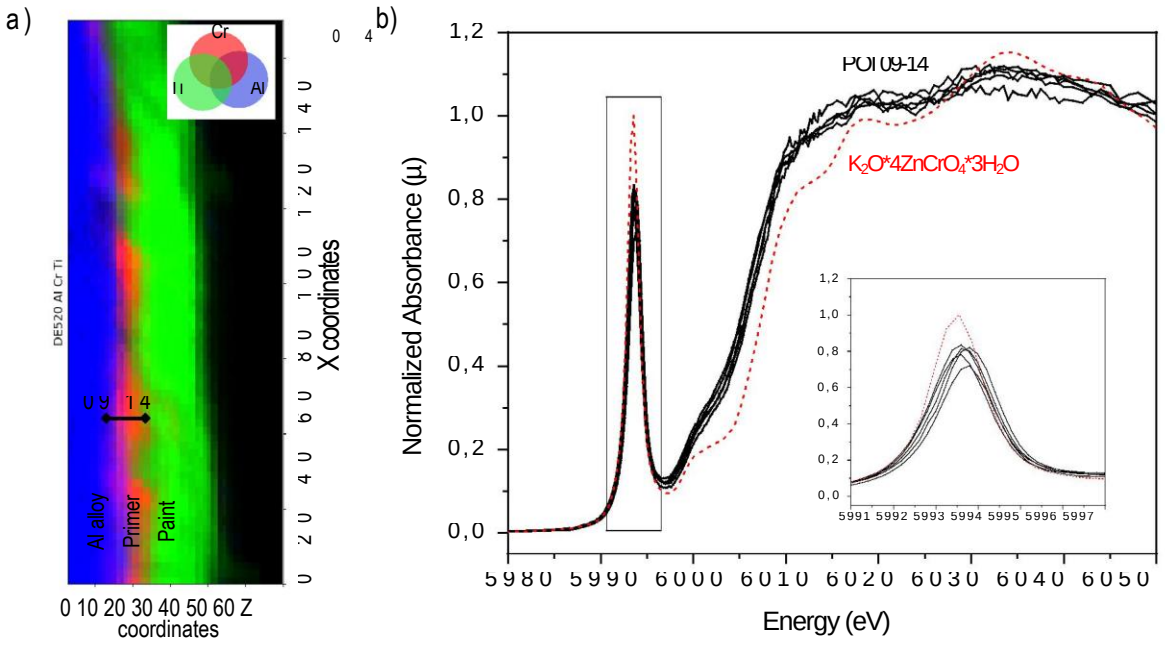

Figure 5. DE520 cross-section sample: a) XRF (Cr, Ti, Al) map revealing the paint layer (green) and the primer (red) on the Al alloy (blue), with POI profile line (from 09 to 14) and b) the corresponding normalised XANES spectra across the Al/primer interface; inset: close-up view of the pre-edge peak at 5993.5 cm-1. Spectrum of the reference zinc yellow pigment K2O*4ZnCrO4*3H2O (courtesy of J.F. Gaillard) is also shown (dashed line).

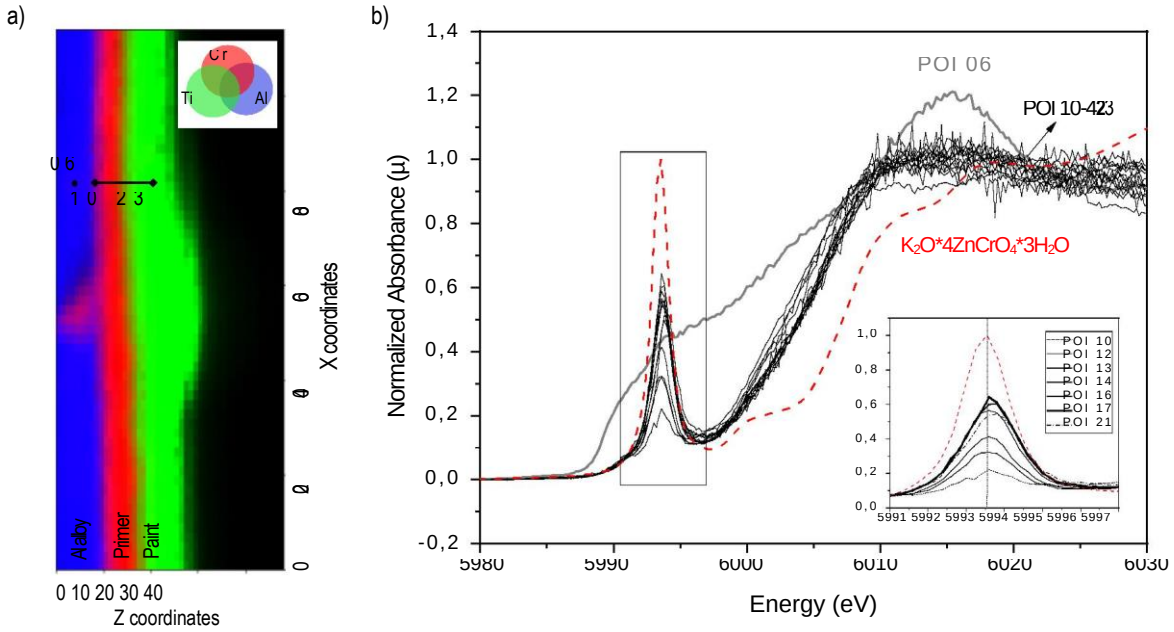

Figure 6. LA298 cross-section sample: a) XRF (Cr, Ti, Al) map with POI 06 (in the Al alloy) and POIs from 10 to 23; b) Normalised XANES spectra across the Al/primer interface:), POI 06 (Al alloy), POI 10-POI 11 (interface); POI 14 (in the middle of the layer) plotted together with that of the reference Zn yellow (dashed line); inset: close-up view of the pre-edge peak.

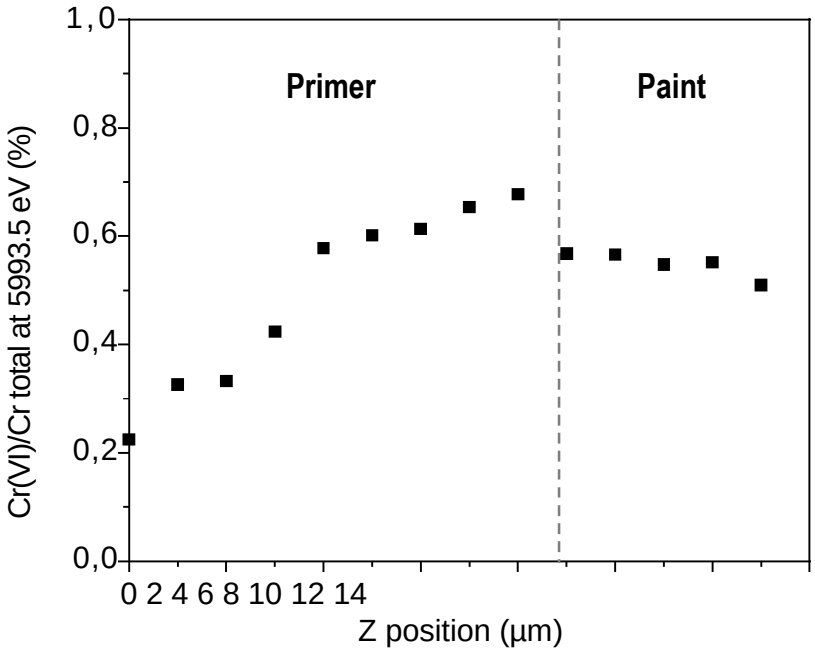

Figure 7. LA298 cross-section sample - Evolution of the Cr(VI) peak intensity at 5993.5 eV normalised to (Cr total) (Hμ(5993)) within the primer from POI 10 (0 µm) to POI 23 (13 µm).

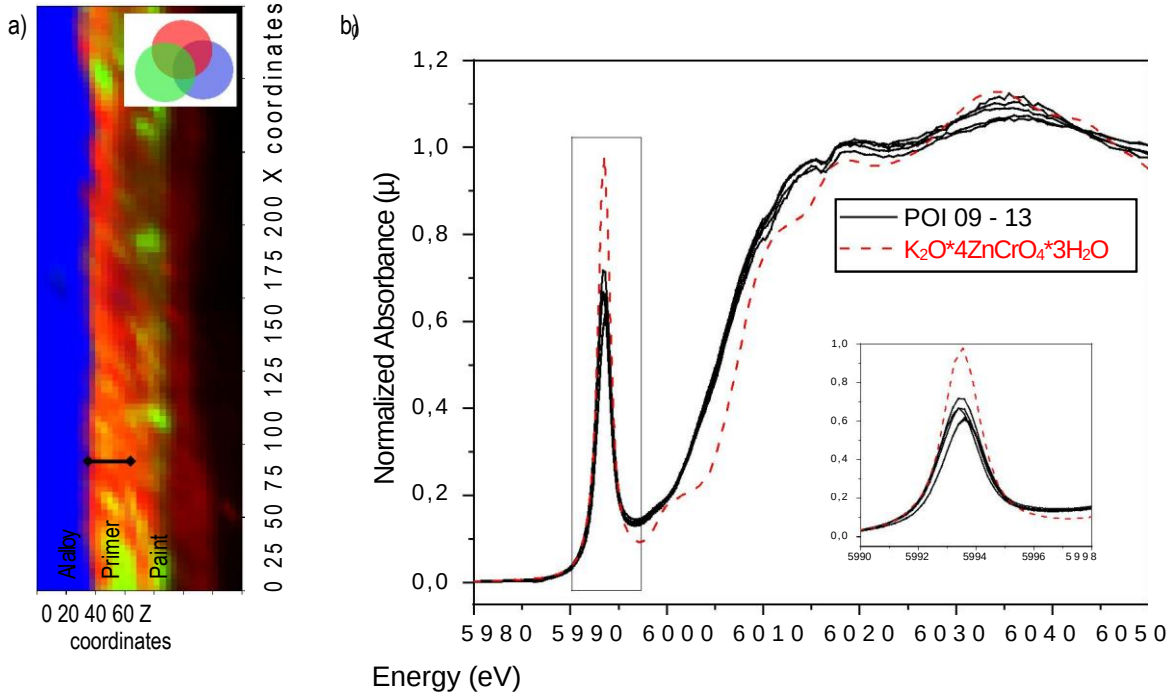

Figure 8. HE111-zone H1 cross section sample: a) XRF (Cr, Si, Al) map with POIs from 09 to 13; b) normalised XANES spectra across the Al/primer interface. The plot for the reference Zn yellow is shown by the dashed line; Inset: close-up view of the pre-edge peak.

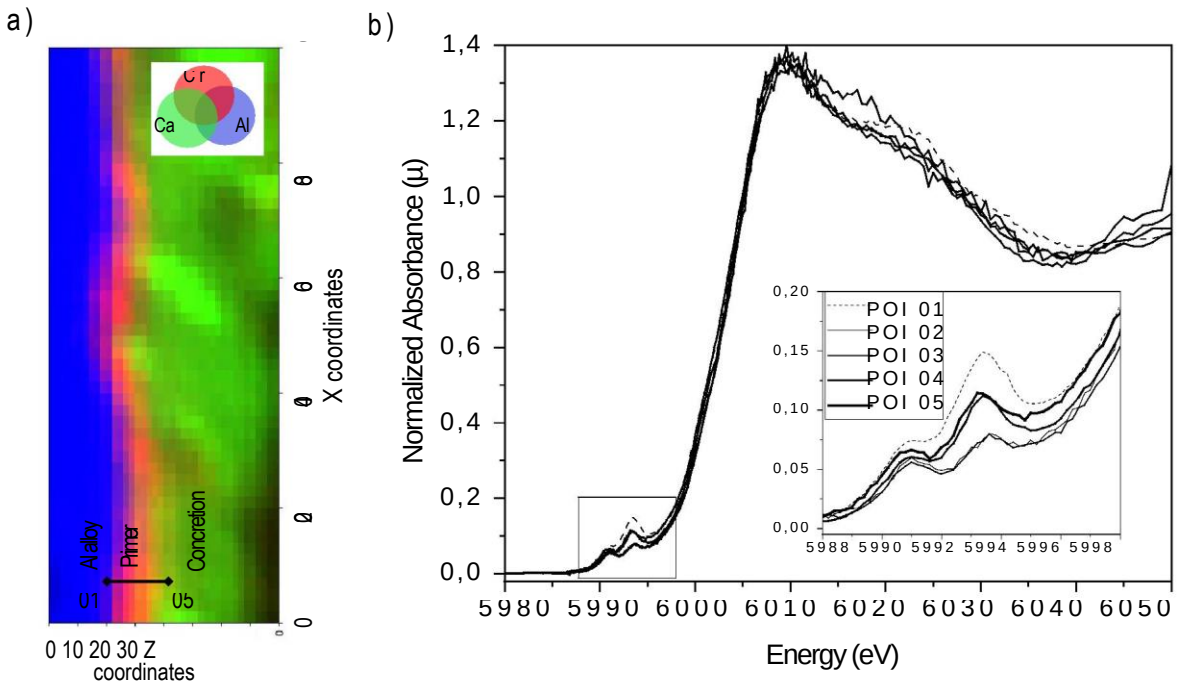

Figure 9. HE111-zone H2 cross-section sample: a) XRF (Cr, Ca, Al) map with POIs from 01 to 05 and b) normalised XANES spectra across the Al/concretion interface; Inset: close-up view of the pre-edge peaks.

Table 1. Elemental composition in normalised weight (wt.%) measured by SEM-EDS analysis on polished cross-sections (estimated error is 10% for minor elements).

Sample	Elemental composition (wt%)								
	Al	**Cu**	**Mg**	**Mn**	**Fe**	**Si**	**Zn**	**Cr**	**Ni**
DE520	93.2	4.4	0.5	0.6	0.3	0.5	--	--	--
LA298	93.3	3.8	0.7	0,0	0.4	0.4	0.5	0.6	0.4
HE111	93.2	4.3	0.6	0.8	0.3	0.5	--	--	--